Pergamon

Bioorganic & Medicinal Chemistry 10 (2002) 1979–1989

BIOORGANIC & MEDICINAL CHEMISTRY

Analysis of Stereoelectronic Properties, Mechanism of Action and Pharmacophore of Synthetic Indolo[2,1-*b*]quinazoline-6,12-dione Derivatives in Relation to Antileishmanial Activity Using Quantum Chemical, Cyclic Voltammetry and 3-D-QSAR CATALYST Procedures

Apurba K. Bhattacharjee,* David J. Skanchy, Barton Jennings,† Thomas H. Hudson, James J. Brendle and Karl A. Werbovetz‡

Division of Experimental Therapeutics, Walter Reed Army Institute of Research, 503 Robert Grant Avenue, Silver Spring, MD 20910, USA

Received 22 May 2001; accepted 12 December 2001

Abstract—Several indolo[2,1-*b*]quinazoline-6,12-dione (tryptanthrin) derivatives exhibited remarkable activity at concentrations below 100 ng/mL when tested against in vitro *Leishmania donovani* amastigotes. The in vitro toxicity studies indicate that the compounds are fairly well tolerated in both macrophage and neuronal lines. An analysis based on qualitative and quantitative structure–activity relationship studies between in vitro antileishmanial activity and molecular electronic structure of 27 analogues of indolo[2,1-*b*]quinazoline-6,12-dione is presented here by using a combination of semi-empirical AM1 quantum chemical, cyclic voltammetry and a pharmacophore generation (CATALYST) methods. A modest to good correlation is observed between activity and a few calculated molecular properties such as molecular density, octanol–water partition coefficient, molecular orbital energies, and redox potentials. Electron transfer seems to be a plausible path in the mechanism of action of the compounds. A pharmacophore generated by using the 3-D QSAR of CATALYST produced a fairly accurate predictive model of antileishmanial activity of the tryptanthrins. The validity of the pharmacophore model extends to structurally different class of compounds that could open new frontiers for study. The carbonyl group of the five- and six-membered rings in the indolo[2,1-*b*]quinazoline-6,12-dione skeleton and the electron transfer ability to the carbonyl atom appear to be crucial for activity.

Introduction

Diseases caused by protozoal parasites have an overwhelming impact on public health throughout the world, particularly in the tropics and subtropics. The leishmaniases represent a spectrum of disease resulting from different species belonging to the genus *Leishmania*, a protozoal parasite transmitted by the bite of the phlebotomine sandfly. Clinical manifestations of the infection range from cutaneous and mucocutaneous to visceral leishmaniasis. An estimated 1.5–2 million new cases of leishmaniasis occur each year, which in the visceral manifestation is often fatal if untreated.[1] An additional 350 million people in 88 countries around the world are threatened by leishmaniasis, and visceral leishmaniasis alone has claimed an estimated 100,000 lives in Sudan in recent outbreaks.[2] Nonavailability of satisfactory chemotherapeutic agents and failure to develop an effective vaccine are considered to be two stumbling blocks in the combat of this disease.[3]

The current chemotherapy of leishmaniasis relies upon the use of pentavalent antimony compounds that require parenteral administration of high doses and a lengthy course of treatment resulting in marked increase of serious side effects and decreasing efficacy. Two pentavalent antimonial drugs, sodium stibogluconate (Pentostam) and meglumine antimonate (Glucantime) are the current treatments of choice for leishmaniases and have been the choice for the past 50 years. Such heavy

*Corresponding author. Tel.: +1-301-319-9043; fax: +1-301-319-9449; e-mail: apurba.bhattacharjee@na.amedd.army.mil (A.K. Bhattacharjee); werbovetz@dendrite.pharmacy.ohio-state.edu (K.A. Werbovetz)

†Present address: Millennium Pharmaceuticals, Inc., 38-2 Sidney Street, Cambridge, MA 02139, USA.

‡Present address: Division of Medicinal Chemistry and Pharmacognosy, College of Pharmacy, The Ohio State University, 500 West 12th Ave., Columbus, OH 43210-1291, USA.

0968-0896/02/$ - see front matter
PII: S0968-0896(02)00013-5

metal pharmacology is found to have side effects such as nausea, diarrhea, convulsions, and even cardiotoxicity.[4] Antimony-resistant strains have also been reported.[5] Thus, there is a clear need for development of less toxic drugs that are effective against all forms of leishmaniases.

Much effort and attention have therefore been focused on the discovery and development of new and less toxic chemotherapeutic agents in recent years.[3,6] Indolo[2,1-*b*]-quinazoline-6,12-dione (tryptanthrin) is a compound with a long history[7] and is well documented to possess antibacterial activity against a variety of pathogenic bacteria, particularly the causative agent of tuberculosis.[8,9] Recently, indolo[2,1-*b*]quinazoline-6,12-dione and its substituted derivatives were revisited in a screening campaign conducted by the Walter Reed Army Institute of Research, Silver Spring, MD (USA). The compounds displayed remarkable in vitro antileishmanial activity against *Leishmania donovani*. Indolo[2,1-*b*]quinazoline-6,12-dione and derivatives can be easily synthesized by various methods that are discussed in a later section. The parent compound can also be produced by *Candida lipolytica* when grown in media containing an excess of tryptophan, hence the name tryptanthrin. To further improve the in vitro activity, a series of additional azatryptanthrin analogues were designed and tested incorporating a pyridine moiety for ring A with one or two nitrogen atoms. Many of these compounds showed high efficacy against *Leishmania*. The present study deals with 27 such analogues (Chart 1) that were tested for in vitro antileishmanial activity against *L. donovani*.

However, the mode of action of these compounds is yet unknown, and very little molecular level information is found in literature to supplement a rational selection of these compounds. Since the ability of drugs to interact with the recognition sites in receptors results from a combination of steric and electronic properties,[10–12] a study of the molecular electronic structure of the indolo[2,1-*b*]quinazoline-6,12-dione derivatives should provide better insights of the mechanism of action of the compounds and aid the design of more efficient analogues. Moreover, a three-dimensional pharmacophore model generation would be useful to identify the structural requirements for antileishmanial activity in this series and also be useful for 3-D queries to search databases of proprietary and/or commercially available compounds. Thus, in continuation of our efforts and interest in the design of antileishmanial chemotherapeutic agents,[6,13,14] we present here a detailed analysis of stereoelectronic properties in relation to structure–activity relationships and mechanism of action of the above 27 tested tryptanthrins using a combination of semi-empirical AM1 quantum chemical,[15] cyclic voltammetry,[16] and 3-D-QSAR CATALYST[17] methods.

Chart 1.

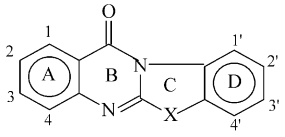

Compd	1-	2-	3-	4-	X	1′	2′	3′	4′
1	CH	–N=	CH	CH	C=O	CH	CH	$CCH(OCH_3)_2$	CH
2	CH	CH	CH	–N=	C=O	CH	CH	C–I	CH
3	CH	–N=	CH	CH	C=O	CH	CH	$C–OCF_3$	CH
4	CH	CH	$CS(CH_2)_2OH$	CH	C=O	CH	CH	C–Cl	CH
5	CH	–N=	CH	CH	C=O	CH	CH	CCH_2OCH_3	CH
6	CH	CH	CH	–N=	C=O	CH	CH	C-Cl	CH
7	CH	CH	CH	–N=	C=O	CH	C–Cl	CH	CH
8	CH	CH	CH	–N=	C=O	CH	CH	$CCO_2CH_2CH_3$	CH
9	CH	–N=	CH	CH	C=O	CH	CH	$CCHOCH_3$–$CH(CH_3)_2$	CH
10	CH	–N=	CCH_3	–N=	C=O	CH	CH	C–Cl	CH
11	CH	CH	C-F	CH	C=O	CH	CH	C–Cl	CH
12	CH	CH	CH	–N=	C=O	CH	CH	C–F	CH
13	CH	–N=	CH	CH	C=O	CH	CH	C–Br	CH
14	CH	CH	$C–N<(CH_2)_4>N–CH_3$	CH	C=O	CH	CH	C–Cl	CH
15	CH	CH	CH	CH	C=O	CH	CH	C–F	CH
16	CH	CH	$C–NCH_3(CH_2)_2OH$	CH	C=O	CH	CH	C–Cl	CH
17	CH	CH	CH	C-F	C=O	CH	CH	C–F	CH
18[a]	CH	CH	CH	CH	C=O	CH	CH	C–F	CH
19	CH	CH	CH	CH	C=O	CH	CH	CH	C-Cl
20	CH	CH	C–N–Cyclohexyl	CH	C=O	CH	CH	C–Cl	CH
21	CH	$C–CH_3$	CH	CH	C=O	CH	CH	C–F	CH
22	CH	CH	CH	CH	C=O	CH	CH	CH	CH
23	CH	CH	CH	$C-OCH_3$	C=O	CH	CH	C–I	CH
24	CH	CH	CH	CH	$C=C(CN)_2$	CH	CH	C–F	CH
25	CH	CH	CH	$C-OCH_3$	C=C–Phenyl	CH	CH	C–F	CH
26	CH	CH	C–F	CH	C=O	CH	$C–N<(CH_2)_4>N–CH_3$	C–F	CH
27	C–Cl	Br	CH	Br	C=O	CH	CH	CH	CH

[a]In this compound, the aromatic N of ring B has been replaced with a N–H group.

Results and Discussion

Antileishmanial activity and toxicity to in vitro mammalian cell lines

Twenty-seven tryptanthrin analogues were screened in vitro against *L. donovani* axenic amastigotes as described previously.[6,12,14] These compounds displayed remarkable antileishmanial activity, with 13 of the agents studied displaying IC_{50} values below 100 ng/mL. Compounds **1** and **2** were the most active against *Leishmania* in this study, with IC_{50} values of 16 ng/mL (Table 1). As a means of comparison, the clinically useful antileishmanial agent amphotericin B possesses an IC_{50} value in this assay of 416 ng/mL.[14] Eighteen of these compounds were also tested for toxicity against murine J774 macrophages and rat neuronal NG-108–15 cells (Table 2). In almost all cases, the tryptanthrins were considerably more toxic to the parasites than to the mammalian cell lines, and were frequently an order of magnitude more active against *L. donovani*. The best selectivity was observed with compound **6**, which was 69-fold more toxic to the parasites than to both mammalian cell lines.

Analysis of stereoelectronic properties

Molecular level information obtained from semi-empirical (AM1) quantum chemical calculations on the optimized electronic structure of the compounds were investigated to explore quantitative as well as qualitative relationships between chemical structure and biological activity in the light of QSAR analysis developed by Hansch.[18] The fundamental hypothesis of QSAR is that biological properties are functions of molecular structure. It is reasonable to assume that certain conformations of a molecule can only bind to the specific site of the receptor. The compounds that have both the necessary functional groups and right conformation will only interact with the target. Thus, molecules with similar structures and electronic properties are likely to have similar biological activity. Accordingly, molecular properties such as (a) the structural parameters, (b) molecular density, (c) log P, (d) molecular orbital energies, and (e) electrostatic potentials were calculated and the results examined.

The fully optimized geometry the molecules indicates that the rings A, B, C, and D in the indolo[2,1-*b*]quinazoline-6,12-dione skeleton are planar and superimposable (data not shown). From a structural point of view, a carbonyl group at the five-membered C ring is an important requirement for potent activity because in the absence of it the activity decreases dramatically (Chart 1, Table 1). Bulkier groups at the 3′-position of the D ring and a nitrogen atom at either the 2- or 4-position of the A ring in the indolo[2,1-*b*]quinazoline-6,12-dione skeleton seem to support potent activity. Steric factors associated with the substitutions at the 3′-position of ring D appear to outweigh the electronic effects for potent antileishmanial activity though the role of electronic effects at this position due to substituents such as F, Cl, Br, I, and OCF_3 cannot be totally discounted. Other calculated molecular properties and the in vitro IC_{50} values against *L. donovani* axenic amastigotes of the compounds are presented in Table 1.

Inspection of Table 1 indicates an increasing trend of activity with increasing molecular density and decreasing octanol/water partition coefficients (log P) for a large number of the tryptanthrin analogues but no quantitative linear relationship could be established between the two properties and activity. However, the observed trend indicates that density and lipophilicity of the molecule may be contributing for potent activity of the compounds. More dense molecules being more potent may imply less susceptibility for metabolic degradation and longer survival time for transport into the parasite infected cells facilitating a better parasite killing in the macrophages. But there remains a concern because this property could impart toxicity to the potent analogues as well. The observed decreasing trend of calculated log P with increasing activity may imply a role of lipophilicity of the compound for potent activity since the ability of a compound to cross biological membranes is frequently related to its octanol/water partition coefficient. The octanol/water partition coefficients (log P) for the analogues were calculated using the Villars's scale as implemented in SPARTAN.[19]

The correlation between activity and orbital energies particularly the lowest unoccupied molecular orbital (LUMO) energy is quite remarkable. Inspection of both Table 1 and Figure 1 indicates that more negative LUMO energy favors potent activity in the tryptan-

Table 1. Experimental antilesihmanial activities of the compounds with calculated molecular properties and redox potential values

Compd	IC_{50} (ng/mL)	Density	Log P	LUMO (eV)	Redox 1 potential (mV)	Redox 2 potential (mV)
1	16	0.948	1.14	−1.69	na	na
2	16	1.289	na	−1.78	−551	−1163
3	24	1.079	2.19	−1.90	−464	−1102
4	28	1.014	3.19	−1.64	−622	−1239
5	32	0.928	1.91	−1.70	−572	−1184
6	36	1.027	2.04	−1.75	−546	−1197
7	41	1.028	2.28	−1.74	−576	−1175
8	41	0.999	1.18	−1.81	−558	−1190
9	57	0.909	2.35	−1.71	−575	−1184
10	60	1.02	1.4	−1.92	na	na
11	85	1.047	3.36	−1.74	−586	−1242
12	88	1.009	1.35	−1.77	−556	−1199
13	98	1.162	na	−1.82	−481	−1090
14	150	0.997	2.35	−1.50	−692	−1324
15	160	0.99	2.55	−1.62	−656	−1335
16	210	0.97	2.10	−1.51	−720	−1334
17	210	1.031	2.54	−1.73	−593	−1219
18	220	0.985	4.90	−5.90	−662	−1335
19	450	1.011	3.28	−1.54	na	na
20	550	0.998	3.38	−1.47	−696	−1348
21	590	0.989	2.98	−1.59	−679	−1334
22	620	0.948	2.80	−1.44	−750	−1405
23	1200	1.241	na	−1.60	−666	−1272
24	1300	0.99	3.92	−2.21	na	na
25	1500	0.937	4.81	−1.34	na	−1105
26	2100	0.972	1.36	−1.66	−744	−1303
27	17000	1.35	na	−1.82	−566	−1159

Redox 1 = oxygen atom of five-membered ring. Redox 2 = oxygen atom of six-membered ring from cyclic voltammetry experiments.

thrins. Although the plot of LUMO energy versus IC_{50} values (Fig. 1) does not indicate an excellent linear correlation ($r^2 = 0.5258$) the trend is quite apparent. Thus, electron affinity of the molecule could be an important factor associated with potent activity. LUMO sites plotted onto the molecular surface show one prominent site by the carbonyl group of the five-membered ring in all the 27 compounds and the shape of the LUMO is found to be large and extended by the carbonyl carbon atom of the five-membered ring in the more potent analogues. The carbonyl oxygen atom at the five-membered ring is critical for potent activity as absence of this carbonyl oxygen atom dramatically reduces activity of the tryptanthrins (Table 1). Therefore, electron transfer from a receptor site to this carbonyl group seems to be a plausible path in the mechanism action of the compounds, as shown in Chart 2. In order to test the hypothesis, we have performed cyclic voltammetry experiments and observed a good correlation between activity and redox potentials as well as LUMO energy and redox potentials, as described in the following section (Table 1).

Cyclic voltammetry

Since electrochemical methods can provide reliable quantitative assessment of electron transfer ability of a molecule,[20] cyclic voltammetry experiments on each of the analogues were performed to measure the redox potentials associated with electron transfer to the oxygen atoms in compounds. Inspection of Table 1 and the plots (Figs 2 and 3) indicate that although a good linear correlation between activity and redox potentials (Fig. 2, $r^2 = 0.5279$; Fig. 3, $r^2 = 0.5686$) is lacking, the trend for less negative redox potentials of the carbonyl oxygen atoms in the five- as well as in the six-membered rings favoring potent activity is clearly indicated. The correlation profile is quite similar to the LUMO versus activity profile of the compounds indicating that electron affinity is likely to be crucial in the mechanism of action for these compounds. Tryptanthrin analogues containing carbonyl groups at the six- and five-membered rings displayed two reversible waves with cathodic and anodic peaks separated by approximately 60 mV indicating two one-electron transfers (Figs 4 and 5). Plots of peak current versus $(\text{scan rate})^{1/2}$ were linear further confirming the reversible nature of the electron transfers. Experimental and molecular modeling data suggest that the more facile (less negative) redox wave (−0.75 V in unsubstituted tryptanthrin) is due to electron transfer at the carbonyl oxygen on the five-membered ring while the more negative wave is due to electron transfer at the carbonyl oxygen on the six-membered ring (−1.4 V in unsubstituted tryptanthrin). This is supported by the observed electrochemical behavior of the tryptanthrin analogues in which the carbonyl on the five-membered ring has been replaced by a benzylic substituent. This compound displays a single irreversible redox wave below −1.1 V (Fig. 5). Thus, the significance of the carbonyl oxygen at the five-membered ring is clearly indicated, its absence dramatically reduces potent activity of the compounds. Substitution at the 3′-position with electron withdrawing substituents has a larger effect on the redox potential of the less negative wave while substitution at the 4-position has a larger effect on the more negative redox potential which lends further support to the assertion that the first wave (less negative) is due to electron transfer at the carbonyl oxygen on the five-membered ring. A fluorine substituent at the 3′-position causes a shift of +94 mV in the first redox potential and +70 mV shift in the second (more negative) redox potential relative to unsubstituted tryptanthrin. A second fluorine substituent added at the 3-position causes an additional +63 mV shift in the first potential and an additional +116 mV shift in the second potential (Fig. 4). The observation that the more facile reduction occurs on the carbonyl oxygen of the five-membered ring while the more negative redox potential is associated with electron transfer at the carbonyl on the six-membered ring is consistent with the calculated LUMO energies and supports the idea that a facile electron transfer to the oxygen atom of the five-membered ring could be a plausible path in the mechanism of action of the compounds. As cyclic voltammetry experiments allow determination of one-electron reduction potentials and LUMO energy reflects electron affinities expressed in terms of one-electron reduction potentials, these compounds are ideal for assessing the ability of simple theoretical methods to reproduce trends in reduction potentials and, therefore, to anticipate activity.[21] Thus, as expected, LUMO energy values calculated for both carbonyl oxygen atoms correlate fairly well with the measured redox potentials with more

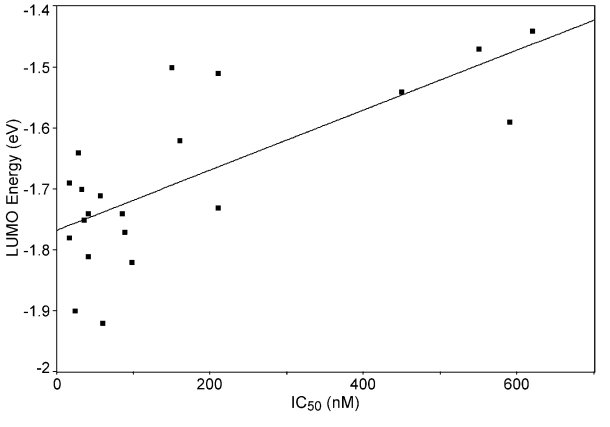

Figure 1. Lowest unoccupied molecular orbital (LUMO) energy against antileishmanial activity of the tyrptanthrins ($r^2 = 0.5258$).

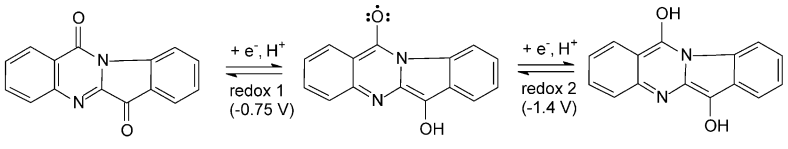

Chart 2.

negative LUMO energies corresponding to less negative redox potentials. The plots of LUMO energy versus the redox potentials of the oxygen atom at the five- and the six-membered rings show linear regression of $r^2 = 0.92$ and $r^2 = 0.85$, respectively (Figs 6 and 7).

3-D-QSAR using CATALYST

The AM1 optimized geometry of 27 indolo[2,1-*b*]quinazoline-6,12-dione analogue was imported from the SPARTAN directory into the CATALYST stockroom to create a training set of antileishmanial tryptanthrins and conformations were generated using the generalized CHARMm force field as implemented in the program. The CATALYST force field has been documented to do better than the semi-empirical quantum chemical methods in predicting the dihedral angles and calculation of conformations of molecules.[22] Molecular flexibility was taken into account by considering each compound as a collection of conformers representing a different area of conformational space accessible to the molecule within a given energy range. The "best quality searching procedure"[17] was adopted to select representative conformers over a 0–25 kcal/mol range above the computed global minimum. Since this search procedure in CATALYST can generate up to 250 conformers for each molecule within 25 kcal/mol conformational energy space above the lowest conformation it can identify the best three-dimensional arrangement of chemical functions explaining the activity variations among the training set. The AM1 calculated bond lengths, valence angles and dihedral angles are found to be in close agreement with molecular force field of the CATALYST (data not shown). A prerequisite for development of a reliable 3-D QSAR model for antileishmanial property of the compounds is the correlation of a characteristic and reproducible biological activity to structural information of the respective compound. The conformational model of the compounds in the training set of 27 tryptanthrins was used for hypothesis (pharmacophore) generation that aims to identify the best three-dimensional arrangement of chemical functions explaining the activity variations among the training set.[23] The training set for the present study was prepared with the in vitro activity data and the automatic generation of hypotheses was performed within CATALYST (HypoGen) using aromatic hydrophobic sites, hydrogen bond acceptor, hydrogen bond acceptor (lipid) and ring aromatic sites as the functional features to describe the antileishmanial activity of the compounds. Calculated stereoelectronic properties of the compounds provided an idea about the pharmacophoric model of the training set and aided in the selection of the functional features in the generation of the hypothesis. It was found that only two of the four features, hydrogen bond acceptor and hydrogen bond acceptor (lipid) are embodied in the statistically most significant hypothesis out of the 10 generated hypotheses (cost = 114.0, fixed cost = 106.3, RMS = 0.71). The RMS values of the other automatically generated hypotheses range between 0.7 and 0.8. The dumping score for the

Table 2. Toxicity profile of the tryptanthrins

Compd	IC_{50}	Mouse macrophage	Neuronal
1	16	850	200
2	16	—	—
3	24	1000	1500
4	28	200	150
5	32	—	—
6	36	2500	2500
7	41	—	—
8	41	1300	925
9	57	200	700
10	60	2500	2500
11	85	200	500
12	88	1550	120
13	98	250	350
14	150	850	120
15	160	—	—
16	210	1500	1000
17	210	1500	2500
18	220	912	560
19	450	—	—
20	550	850	120
21	590	850	170
22	620	—	—
23	1200	400	625
24	1300	1500	2500
25	1500	—	—
26	2100	—	—
27	17000	—	—

All values are given in ng/mL.

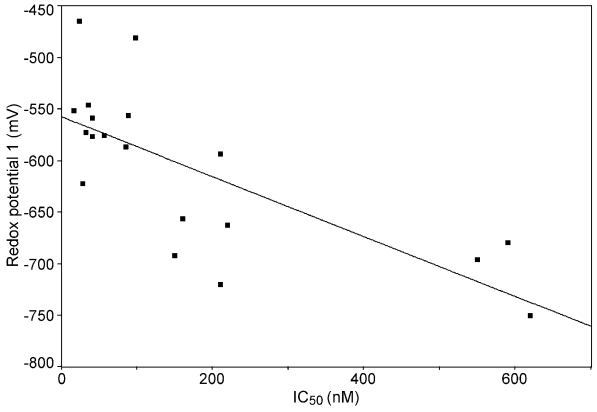

Figure 2. Redox potential of the carbonyl oxygen in the five-membered ring versus antileishmanial activity of the tryptanthrins ($r^2 = 0.5279$).

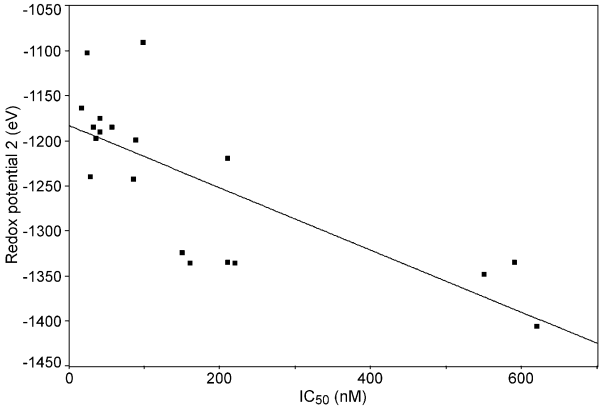

Figure 3. Redox potential of the carbonyl oxygen in the six-membered ring versus antileishmanial activity of the tryptanthrins ($r^2 = 0.5686$).

null hypothesis was 123.4. The total costs of the 10 generated hypotheses varied over a range between 114.0 and 121.0, eight of them in a narrow range of 114.0 to 114.23. This cost factor, known as *Config*, is a measure of the magnitude of the hypothesis space for a given training set of compounds. If the value exceeds 17, there are more degrees of freedom in the training set that CATALYST algorithm can properly handle and the hypothesis result is likely to be poor.[24,25] The *Config* values of the 10 generated hypotheses for the present training set were 14.78. One of the most potent analogues of the training set such as, **2** maps very well with the statistically most significant hypothesis (Fig. 8) whereas, the least potent analogue of the series such as, **27** does not map adequately with the hypothesis (Fig. 9). The critical hydrogen bond acceptor profile by the carbonyl oxygen at the five-membered ring in the hypothesis appears to be consistent with the above stereoelectronic analyses where it is clearly shown that absence of the five-membered carbonyl oxygen atom will dramatically reduce potent activity of the tryptanthrins. Table 3 summarizes the estimated as well as the measured IC_{50} values for the training set along with the error values. The error column in Table 3 represents the ratio of the estimated activity to measured activity, or its negative inverse if the ratio is less than one. Plot of the experimental activity values versus the calculated activity of the training set gave a fairly good correlation ($=0.89$) between the experimental activity (true activity) and estimated activity (Fig. 10). Although the plot shows two concentrated areas of clustered IC_{50} values indicating some redundancy in the structural and activity information to CATALYST we attempted to test the validity of the hypothesis over the entire training set of 27 compounds. However, removal of some of the above redundancy of structure and activity information from the training set did not appear to produce any better correlation though the plot looked more spread-out (data not shown).

In order to cross-validate the observed correlation we have prepared a test training set of 14 other tryptanthrins (Chart 3) that were tested for antileishmanial activity in the identical assay by screening in vitro against *L. donovani* like the original training set. Moreover, this test set of the tryptanthrins has never seen before the CATALYST (HypoGen) hypothesis model that we have generated with the original training set. A regression analysis was performed with the test set compounds and the best hypothesis generated from the

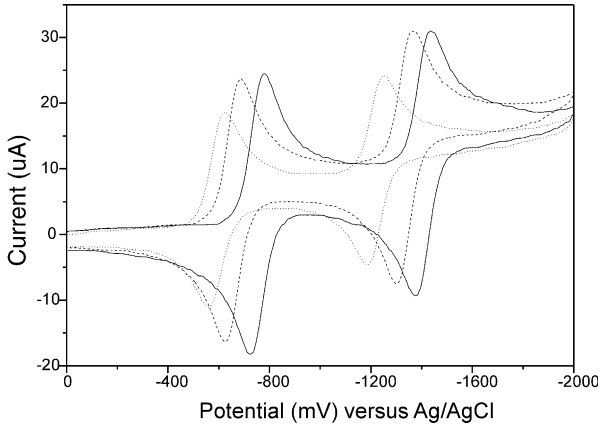

Figure 4. Superimposed cyclic voltammograms of tryptanthrin (**22**, solid), 3′-flouro tryptanthrin (**15**, dashed), 3′,4-flouro tryptanthrin (**17**, dotted) showing the effect of electron withdrawing substituents on the redox potentials. All scans are shown at a scan rate of 50 mV/s.

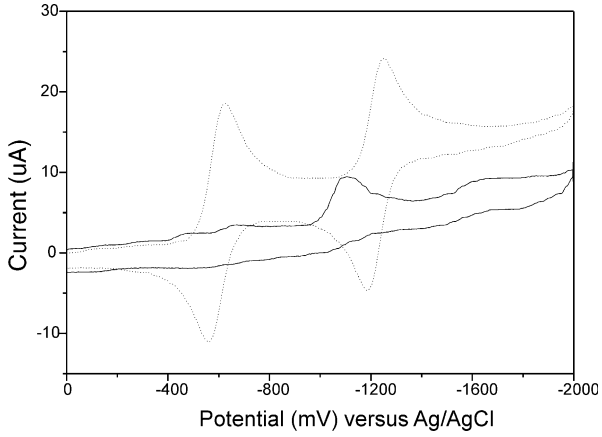

Figure 5. Superimposed cyclic voltammograms of compound **25** (solid) and 3′,4-flouro tryptanthrin (**17**, dotted) showing the effect of replacing the five-membered ring carbonyl moiety with a benzylic substituent. Both scans shown are at a scan rate of 50 mV/s.

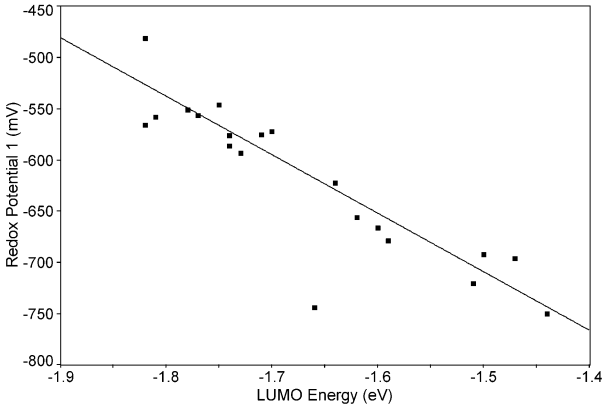

Figure 6. LUMO energy against redox potential of the carbonyl oxygen in the five-membered ring with linear regression line ($r^2=0.9238$).

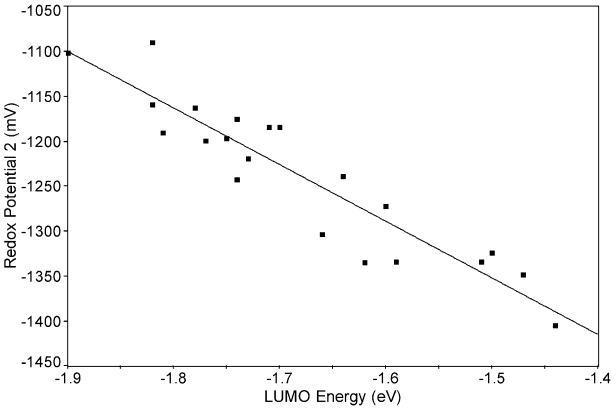

Figure 7. LUMO energy against redox potential of the carbonyl oxygen in the six-membered ring with linear regression line ($r^2=0.8584$).

original training set and a correlation close to 0.8 is observed between true activity and the estimated activity values. The estimated as well as the measured IC_{50} values for the test set tryptanthrins along with the error values are also presented in Table 3. The actual activity values are reproduced reasonably well within the limits of uncertainty (Table 3), thus indicating a good predictive power of the original hypothesis or pharmacophore. The more potent analogue in the test set of tryptanthrins such as **1′** maps well with the original hypothesis whereas, the less potent analogues such as **6′** and **14′** do not map adequately with the hypothesis.

Using the generated hypothesis, we have performed a database search for potential new antileishmanial candidates from our in-house Chemical Information System[26] database of over 240,000 compounds. The Chemical Information System database was built as a multi-conformer database in CATALYST using the catDB utility program as implemented in the software. The catDB format allows a molecule to be represented by a limited set of conformations thereby permitting conformational flexibility to be included during the database search. However, the search resulted in the identification of more than 300 compounds, and therefore required further refinement of our hypothesis in order to have a shorter list of potential lead compounds. The refinement was done by incorporating a few additional features that were observed from the results of quantum chemical calculations such as a critical vector direction or electric field direction for the hydrogen bond acceptor and the presence of hydrophobic aromatic rings from the electrostatic potential profiles. A database query was thus formulated by superimposing the in vitro hypothesis and a conformer of **1**, one of the two most potent analogues. Three positional constraints for the sites of the functional features were incorporated and the molecule was transformed into a 3-D shape with all the functional features that are believed to be associated with potent activity. The final query now contains a 3-D shape with three position constraints representing two hydrogen bond acceptors (lipid), a hydrogen bond acceptor with a direction vector, and a ring aromatic (Fig. 11). Using this query as the template for search, the in-house CIS database led to the discovery of 43 compounds. Interestingly, 16 compounds from the list were found to be positively active ($IC_{50} < 2000$ ng/mL) as antileishmanials in our parasite drug susceptibility assay. We have identified two com-

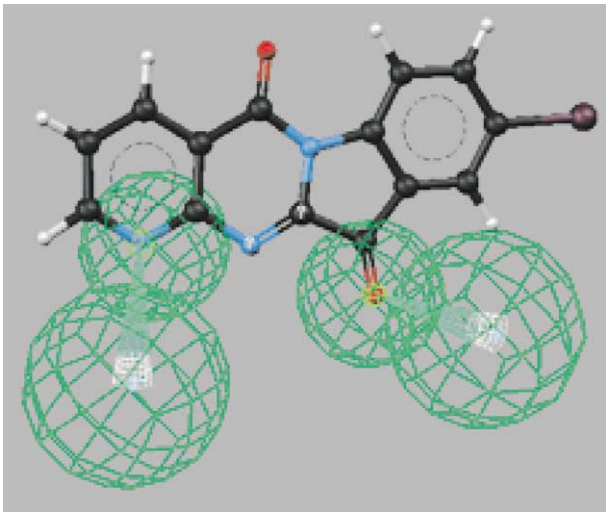

Figure 8. Mapping of one of the two most potent members of the training set, compound **2**, onto the statistically most significant hypothesis.

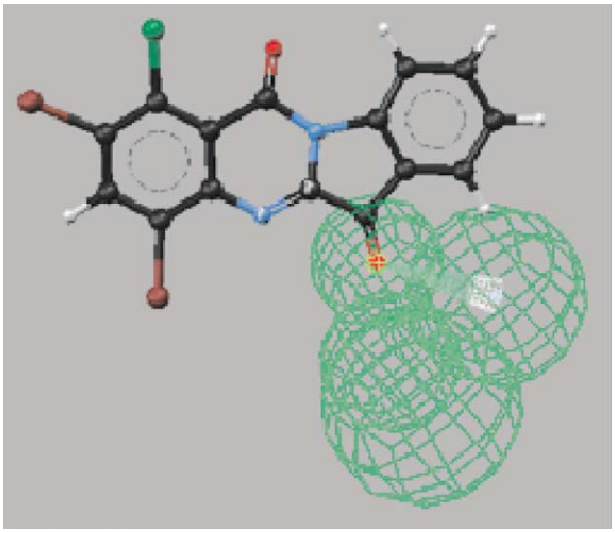

Figure 9. Mapping of the least potent member of the training set, compound **27**, onto the statistically most significant hypothesis.

Table 3. Estimated and experimentally determined activity values of the training set and the test set of the compounds

Training set (compd)	IC_{50} (expt)	IC_{50} (est)	Error[a]	Test set (compd)	IC_{50} (expt)	IC_{50} (est)	Error[a]
1	16	30	1.9	**1′**	11	20	1.8
2	16	41	2.6	**2′**	26	20	−1.3
3	24	40	1.7	**3′**	40	20	−2.0
4	28	53	1.9	**4′**	53	110	2.1
5	32	46	1.4	**5′**	64	270	4.2
6	36	41	1.1	**6′**	147	870	5.9
7	41	41	−1.0	**7′**	173	840	4.8
8	41	42	1.0	**8′**	636	850	1.3
9	57	34	−1.7	**9′**	822	900	1.1
10	60	39	−1.5	**10′**	1012	830	−1.2
11	85	390	4.6	**11′**	1218	1110	−1.1
12	88	41	−2.1	**12′**	1434	860	−1.7
13	98	240	2.4	**13′**	2146	840	−2.5
14	150	300	2.1	**14′**	3817	860	−4.5
15	160	450	2.8				
16	210	440	2.1				
17	210	180	−1.9				
18	220	450	2.0				
19	450	390	−1.1				
20	550	400	−1.4				
21	590	430	−1.4				
22	620	430	−1.5				
23	1200	360	−3.3				
24	1300	2500	1.9				
25	1500	370	−4.0				
26	2100	330	−6.4				
27	170,000	5600	−2.9				

IC_{50} all values are given in ng/mL.
[a]Values in the error column represent the ratio of the estimated activity to measured activity, or its negative inverse if the ratio is less than one.

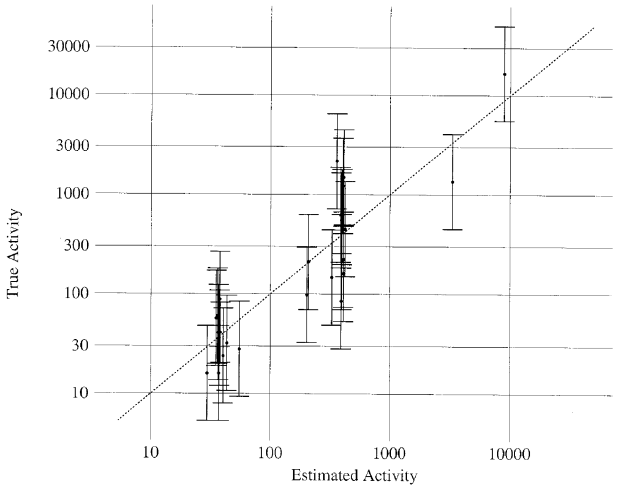

Figure 10. Plot displaying the experimental IC_{50} values (ng/mL) versus IC_{50} values estimated by using the statistically most significant hypothesis derived from the training set of 27 tryptanthrins (correlation coefficient = 0.8943).

pounds, **28** (7-oxo-7*H*-benzo/e/pyrimidine-4-carboxylic acid) (IC_{50} = 754 ng/mL) and **29** (1,4,5-trihydroxy anthraquinone) (IC_{50} = 1806 ng/mL) from the list that have shown potentials for further study (Chart 4). We are currently employing these two compounds as new antileishmanial leads starting from structural modifications to synthesis, design of new analogues and testing.

Although the tryptanthrins possess outstanding activity against axenic *L. donovani* amastigotes, these agents have yet to display activity in *Leishmania* infected cells,[27] a model which is a better predictor of in vivo antileishmanial activity than the axenic amastigote assay. We are continuing to explore new strategies to translate the potent intrinsic antileishmanial activity of the tryptanthrins into new candidates for treating leishmaniasis. We have currently undertaken metabolic stability and Caco-2 permeability studies and exploring the possibility of developing pharmacophore models on the ADME properties of the compounds from the experimental data.

Conclusion

The study organizes the molecular characteristics that are both statistically and mechanistically significant for potent antileishmanial activity from a set of diverse indolo[2,1-*b*]quinazoline-6,12-dione derivatives. Stereoelectronic factors of the substituents at the 3′-position of the D ring in indolo[2,1-*b*]quinazoline-6,12-dione skeleton appear to have significant effect on potent activity. The carbonyl groups of the five- and six-membered rings in the tryptanthrin moiety and electron transfer ability from a receptor is likely to be a crucial step in the mechanism of action in the compounds. The presence of a five-membered carbonyl moiety in the molecule appears to be a structural requirement for potent activity. Cyclic voltammetry experiments are clearly in agreement with the quantitative as well as qualitative structure activity analyses of the compounds. The chemically significant molecular characteristics disposed in a three dimensional space generated a hypothesis that is found to be quite satisfactory in correlating true activity and estimated activity of the tryptanthrins. The critical hydrogen bond acceptor profile by the carbonyl oxygen at the five-membered ring in the generated pharmacophore is consistent with the stereoelectronic and redox potential analyses of structure–activity of the compounds. The validity of the hypothesis extends to structurally different class of compounds opening new frontiers for study. The compounds are found to be less toxic to mammalian cell lines than to *Leishmania* in vitro. Thus, tryptanthrins show remarkable promise for further study as potential antileishmanial candidates.

Chart 3.

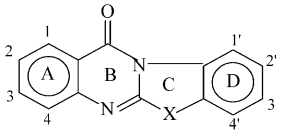

Compd	1-	2-	3-	4-	X	1′	2′	3′	4′
1′	CH	N=	CH	–N=	C=O	CH	CH	CH	CH
2′	–N=	CH	CH	–N=	C=O	CH	CH	CH	CH
3′	CH	–N=	CH	CH	C=O	CH	CH	1,3-Dioxane-2-yl	CH
4′	CH	–N=	CH	CH	C=O	CH	CH	$C–(CF_3)_2–OH$	CH
5′	CH	–N=	CH	CH	C=O	CH	CH	CCH_2OCH_3	CH
6′	CH	CH	$C–N<(CH_2)_4>N–CH_3$	CH	C=O	CH	CH	C–Cl	CH
7′	CH	C–F	C—N$<(CH_2)_4CH_3>$NH	CH	C=O	CH	C-Cl	C–I	CH
8′	CH	CH	$C–N<(CH_2)_4>N–CH_3$	CH	C=O	CH	CH	C–F	CH
9′	CH	$–NH_2$	CH	CH	C=O	CH	CH	C–F	CH
10′	CH	C–F	$C–N<(CH_2)_4>N–COOC(CH_3)_3$	CH	C=O	CH	CH	C–I	CH
11′	CH	CH	CH	$–OCH_3$	C=O	CH	CH	C–I	CH
12′	CH	CCH_3	CH	CH	C=O	CH	CH	CH	CH
13′	CH	CH	C–F	CH	C=O	CH	$C–N<(CH_2)_4>N–CH_3$	C–F	CH
14′	CH	CCH_3	CH	CCH_3	C=O	CH	CH	C–F	CH

Experimental

Chemistry

Indolo[2,1-*b*]quinazoline-6,12-dione and its derivatives were obtained from PathoGenesis Corporation, Seattle, WA, USA (now owned by Chiron, Emeryville, CA, USA). In general, the compounds can be synthesized by base-catalyzed condensation of substituted isatins and substituted isatoic anhydrides through a convenient one-step flexible synthesis as previously reported.[28]

Indolo[2,1-*b*]quinazoline-6,12-dione (22). General method of preparation: isatin (7.35 g) and isatoic anhydride (8.15 g) were added to a well-stirred solution of *N*-methylpiperidine (0.2 mL) and diisopropyl carbodiimide (5 mL) in dry pyridine (35 mL) at 60–65 °C. A clear solution was quickly obtained followed shortly by brisk evolution of CO_2. When the evolution subsided the temperature was slowly (during 10 min) increased to 75 °C. During this operation tryptanthrin starts crystallizing. To complete the reaction a final heating period (30 min) at 95–100 °C is required. Finally the mixture was cooled and the crystals collected, washed with MeOH and dried, yield 11.53 g (93%), mp 267–268 °C (lit. mp 265–266 °C). Without the drying agent the yield drops to 68%. Recently two other methods were reported on the synthesis of tryptanthrins. The first method involves a cyclization of 3-(*o*-chlorophenyl)-2-methyl-4(3*H*)-quinazoline and its meta isomer in liquid ammonia to yield indolo[2,1-*b*]quinazoline-12(6*H*)-one which was oxidized to indolo[2,1-*b*]quinazoline-6,12-dione.[29] The other reported method involves a short-step synthesis as quinazoline alkaloids containing indole skeleton via intramolecular aza-Wittig reaction.[30] Indolo[2,1-*b*]quinazoline-6,12-dione is also a naturally occurring compound was isolated from the Taiwanese medicinal plant, *Strobilanthes cusia* and from *Polygonum tinctorum* and *Isatis* tinctorum.[31] It is produced by *C. lipolytica* when grown in media containing an excess of tryptophan.[32]

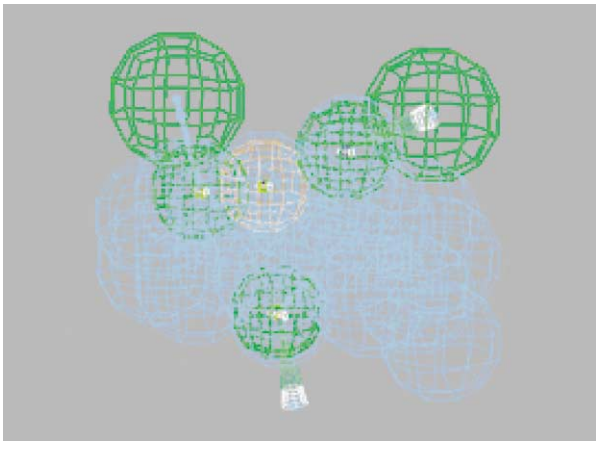

Figure 11. Display of the shape based query for searching the in-house CIS database. The essential elements are one hydrogen bond acceptor on the nitrogen atom of ring A, two hydrogen bond acceptors in the two oxygen atoms, and a hydrophobic function positioned in 3-D space with respective location constraints for a candidate having high antileishmanial activity.

Parasite drug susceptibility assay

Chemicals. Tissue culture media, supplements and chemicals were obtained from the Sigma Chemical Company. Stock solutions of compounds were prepared in DMSO and stored at −30 °C.

Cell lines. *L. donovani* (WHO designation: MHOM/SD/62/1S-CL2$_D$) axenic amastigotes were maintained in modified RPMI medium as previously described.[14]

***Leishmania* drug susceptibility assays.** The growth susceptibility of *L. donovani* amastigote-like forms to the compounds was measured in a three day assay using the CellTiter 96 Aqueous Non-Radioactive Cell Proliferation Assay Kit (Promega) as previously described.[14] A SpectraMax Plus microplate reader (Molecular Devices, Sunnyvale, CA, USA) was used to measure the absorbance in each well at 490 nm. IC values (the concentration of the compound that inhibited parasite growth by 50%) were determined with the software program SoftMax Pro (Molecular Devices) using the dose–response equation $y = ((a-d)/(1+(x/c)^b)) + d$, where x = the drug concentration, y = absorbance at 490 nm, a = upper asymptote, b = slope, c = IC and d = lower asymptote.

Toxicity studies using mouse macrophage and neuronal cells

The toxicity in vitro study was performed against two mammalian cell lines. A subclone (G8) of the murine monocyte-like macrophage line J774 was obtained from Dr. Jose Alunda; Departmento de Sanidad Animal, Facultad de Veterinaria, Universidad Complutense, Madrid, Spain. Murine cells were maintained in 75-cm^2 tissue culture flasks in Dulbecco's modified Eagle medium (GIBCO) supplemented with 10% fetal calf serum, 2 mM L-glutamine 50 μg/mL gentamicin under humidified 5% CO_2/95% air at 37 °C. A subclone (NG-108-15) of a hybrid rat neuroblastoma/mouse glioma cell line was the gift of Dr. Marshall Nirenberg; National Heart Lung and Blood Institute, National Institute of Health, Bethesda, MD, USA. Neuronal cells were maintained in 75-cm^2 tissue culture flasks in Dulbecco's modified essential medium including hypoxanthine-aminopterin-thymidine (HAT) supplement, 10% fetal calf serum and 50 μg/mL gentamicin under humidified 5% CO_2/95% air at 37 °C. Toxicity tests were performed in 96-well tissue culture plates using the protein-binding dye Sulforhodamine B (SRB) as described.[33] Test compounds were serially diluted and added to empty wells of the 96-well plate. Appropriate cells in their respective culture

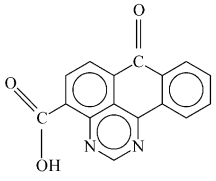

28

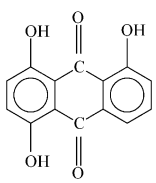

29

Chart 4.

medium were immediately seeded into the wells. Appropriate solvent blanks (no compound) were run in each test. After 72 h under culture conditions, cells were fixed to the plate by layering 50% TCA (4 °C) over the growth media in each well to produce a final TCA concentration of 10%. After incubating for 1 h at 4 °C, cultures were washed five times with tap water and air-dried. Wells were stained for 30 min with 0.4% (w/v) SRB in 1% acetic acid and washed four times with 1% acetic acid. Cultures were air-dried and bound dye was solubilized with 10 mM Tris base (pH 10.5) for 15 min on a gyratory shaker at room temperature. The optical density (OD) at wavelengths of 490–530 nm was then measured with the aid of the SpectraMax Plus microplate reader.

Computational procedure

Computational calculations at the semi-empirical AM1 level were performed using SPARTAN version 5.0[19] running on a Silicon Graphics Octane workstation. Conformational search on each of the 27 analogues was performed by multiple rotations of single bonds in the compounds, thereby generating several low energy conformers with varying population densities. The most abundant and the lowest energy conformers were identified. The geometry of these conformers was optimized, and the electronic properties were calculated using the optimized geometry. Geometry optimization and energy calculations were performed on the compounds in the gaseous phase using AM1 semi-empirical quantum chemical[15] method as implemented in SPARTAN.

Cyclic voltammetry

Cyclic voltammetry experiments were performed on a CV-50W Voltammetric analyzer with a C2 cell stand (Bioanalytical systems, West Lafayette IN, USA). A glassy carbon working, a silver–silver chloride reference electrode and a platinum auxiliary electrode were used in a 5 mL glass cell. All samples were dissolved in dry acetonitrile (Aldrich, St. Louis, MO, USA) with 0.1 M tetrabutylammonium hexafluorophosphate (Aldrich) as the supporting electrolyte. Each tryptanthrin analogue was prepared at a concentration of 1 mM and was degassed with nitrogen for 5 min prior to analysis. Samples were run at several scan rates ranging from 20 to 1000 mV/s.[16] Linear regression analysis of LUMO energy against the redox potential of the carbonyl oxygen was done using TableCurve 2D (SPSS Inc., Chicago, IL, USA).

3-D-QSAR analyses using CATALYST

The software allows the use of structure and activity data for a set of lead compounds to create a hypothesis characterizing the activity of the lead set. The AM1 optimized geometry of each of the 27 tryptanthrins was imported in CATALYST and was minimized to the closest local minimum using molecular mechanics based CHARMm force field. Conformational models were generated that emphasize representative coverage over a 0–25 kcal/mol range above the computed global minimum. CATALYST algorithm allows a conformational search generating up to 250 conformers for each molecule within 25 kcal/mol conformational energy above the global minimum energy conformation. The conformational model of the training set thus used for hypothesis (pharmacophore) generation should be better equipped to identify the best three-dimensional arrangement of chemical functions explaining the activity variations among the training set. A pharmacophore search was carried out by setting the default parameters used in the automatic generation of hypothesis in CATALYST,[17] such as function weight 0.302, mapping coefficient 0, resolution 297 pm, and activity uncertainty 3. Hypotheses approximating the pharmacophore of the tryptanthrins are described as a set of functional features such as aromatic hydrophobic, hydrogen bond acceptor, hydrogen bond acceptor lipid, positively and negatively ionizable sites distributed within a 3-D space. These functional features are represented either by points or vector geometrical objects. The direction of the vector representing a functional feature of an atom, for example the features associated with hydrogen bonding, is determined from the symmetry, the number of localized lone pairs, the extended effect of the lone pairs from their electrostatic potential profiles, and the environment surrounding the atom. There are two primary methods of generating a hypothesis within CATALYST. The first method is to interactively build hypotheses by one of several procedures available in the 'view hypothesis' workbench based upon the significance of the chemical functions and fragments comprising the target molecule. The other method automatically generates a hypothesis from a diverse set of lead compounds that have activity data from the same assay. We have used both the methods. The statistical relevance of various generated hypotheses is assessed on the basis of the cost relative to the null hypothesis and the correlation coefficients. The hypotheses are then used to estimate the activities of the training set. These activities are derived from the best conformation generation mode of the conformers displaying the smallest root-mean square (RMS) deviations when projected onto the hypothesis.

Acknowledgements

The authors wish to acknowledge Dr. William Baker and Pathogenesis Corporation, Seattle, WA 98119, USA for providing the compounds used in this study under a cooperative research agreement. We thank Dr. Shikha Varma of Accelrys, Burlington, MA 01803, USA for reading the manuscript and providing valuable suggestions. We also acknowledge COL John P. Scovill for his efforts in obtaining the compounds.

References and Notes

1. World Health Organization. http://www.who. int/emc/diseases/leish/leisdis1.html, 2000.
2. Seaman, J.; Mercer, A.; Sondorp, E. *Int. J. Epidemiol* **1996**, *25*, 862.
3. Werbovetz, K. *Curr. Med. Chem.* **2000**, *7*, 835.

4. (a) Cook, G. C. *J. Antimicrob. Chemother.* **1993**, *31*, 327. (b) Olliaro, P. L.; Bryceson, A. D. M. *Parasitol. Today* **1993**, *9*, 323.
5. Sacks, D.; Kenney, R.; Kreutzer, R.; Jafffe, C.; Gupta, A.; Sharma, M.; Sinha, S.; Neva, F.; Saran, R. *Lancet* **1995**, *345*, 959.
6. Pitzer, K. K.; Werbovetz, K. A.; Brendle, J. J.; Scovill, J. P. *J. Med. Chem.* **1998**, *41*, 4885.
7. Bird, C. W. *Tetrahedron* **1963**, *19*, 901.
8. Mitscher, L. A.; Wong, W. C.; DeMeulenaere, T.; Sulko, J.; Drake, S. *Heterocycles* **1981**, *15*, 1017.
9. Baker, W. R.; Mitscher, L. A. US Patent 5, 441, 955, 1995.
10. Bhattacharjee, A. K.; Karle, J. M. *J. Med. Chem.* **1996**, *39*, 4622.
11. Bhattacharjee, A. K.; Majumdar, D.; Guha, S. *J. Chem. Soc., Perkin Trans. 2* **1992**, 805.
12. Werbovetz, K. A.; Bhattacharjee, A. K.; Brendle, J. J.; Scovill, J. P. *Bioorg. Med. Chem.* **2000**, *8*, 1741.
13. Bhattacharjee, A. K.; Intl, J. *Quant. Chem.* **1999**, *75*, 995.
14. Werbovetz, K. A.; Brendle, J. J.; Sackett, D. *Mol. Biochem. Parasitol.* **1999**, *98*, 53.
15. Dewar, M. J. S.; Zoebisch, E. G.; Horsley, E. F.; Stewart, J. J. P. *J. Am. Chem. Soc.* **1985**, *107*, 3902.
16. Smyth, M. R.; Vos, J. G. *Analytical Voltammetry*; Elsevier: New York, 1992; Chapter 1.
17. *CATALYST Version 4.5*; Accelrys: San Diego, CA, 1999.
18. Hansch, C. A. *Acc. Chem. Res.* **1969**, *2*, 232.
19. *SPARTAN SGI Version 5.1.2*; Wavefunction Inc.: Irvine, CA, 1998.
20. Chen, H. Y.; Chen, Y.; Zhu, S. M.; Bian, N. S.; Shan, F.; Li, Y. *Talanta* **1999**, *48*, 143.
21. Hehre, W. J.; Burke, L. D.; Shusterman, A. J.; Pietro, W. J. *Experiments in Computational Chemistry*; Wavefunction: Irvine, CA, 1993; Chapter 3.
22. Grigorov, M.; Weber, J.; Tronchet, M. J.; Jefford, C. W.; Milhous, W. K.; Maric, D. *J. Chem. Inf. Comput. Sci.* **1995**, *35*, 285.
23. Baringhaus, K.-H.; Matter, H.; Stengelin, S.; Kramer, W. *J. Lipid Res.* **1999**, *40*, 2158.
24. Greenidge, P. A.; Weiser, J. *Mini Rev. Med. Chem.* **2001**, *1*, 79.
25. Kurogi, Y.; Güner, O. *Curr. Med. Chem.* **2001**, *8*, 1035.
26. *Chemical Information System*; Division of Experimental Therapeutics, Walter Reed Army Institute of Research: Silver Spring, MD 20910, 1999.
27. Brendle, J. unpublished data.
28. Mitscher, L. A.; Wong, W. C.; DeMeulenaere, T.; Sulko, J.; Drake, S. *Heterocycles* **1981**, *15*, 1017.
29. Staskun, B.; Wolfe, J. F. S. *Afr. J. Chem.* **1992**, *45*, 5.
30. Eguchi, S.; Takeuchi, H.; Matsushita, Y. *Heterocycles* **1992**, *33*, 153.
31. Mitscher, L. A.; Drake, S.; Gollapudi, S. R.; Okwute, S. K. *J. Nat. Prod.* **1987**, *50*, 1025.
32. Fiedler, E.; Fiedler, H. P.; Gerhard, A.; Keller-Schierlein, W. *Arch. Microbiol.* **1976**, *107*, 249.
33. Skehan, P.; Storeng, R.; Scudiero, D.; Monks, A.; McMahon, J.; Vistica, D.; Warren, J. T.; Bokesch, H.; Kenney, S.; Boyd, M. R. *J. Natl. Cancer Inst.* **1990**, *82*, 1107.